Life cycle assessment and feasibility analysis of a combined chemical looping combustion and power-to-methane system for CO_2 capture and utilization

P. Bareschino [a,*], E. Mancusi [a], M. Urciuolo [b], A. Paulillo [c,d], R. Chirone [c], F. Pepe [a]

[a] *Dipartimento di Ingegneria, Università Degli Studi Del Sannio, P.zza Roma 21, 82100, Benevento, Italy*
[b] *Istituto di Ricerche Sulla Combustione, Consiglio Nazionale Delle Ricerche, P.le V. Tecchio 80, 80125, Napoli, Italy*
[c] *ELoop S.r.l.V.le A, Gramsci 17/B, 80122, Napoli, Italy*
[d] *Department of Chemical Engineering, University College London, Torrington Place, WC1 E7JE, London, United Kingdom*

ARTICLE INFO

ABSTRACT

The ability to store effectively excess of electrical energy from peaks of production is key to the development of renewable energies. Power-To-Gas, and specifically Power-To-Methane represents one of the most promising option. This works presents an innovative process layout that integrates Chemical Looping Combustion of solid fuels and a Power-to-Methane system. The core of the proposed layout is a multiple interconnected fluidized bed system (MFB) equipped with a two-stage fuel reactor (t-FR). Performances of the system were evaluated by considering a coal as fuel and CuO supported on zirconia as oxygen carrier. A kinetic scheme comprising both heterogeneous and homogeneous reactions occurring in the MFB was considered. The methanation unit was modelled developing a thermodynamic calculation method based on minimization of the free Gibbs energy. The performance of the system was evaluated by considering that the CO/CO_2 stream coming from the t-FR reacts over Ni supported on alumina catalyst with a pure H_2 stream generated by an array of electrolysis cells. The number of cells to be stacked in the array was evaluated by considering that a constant H_2 production able to convert the whole CO/CO_2 stream produced by the CLC process should be attained. The environmental performance of the proposed process was quantified using the Life Cycle Assessment (LCA) methodology. The analysis shows i) that the majority originate from the production and disposal of the oxygen carrier used in the t-FR, and ii) that reusing part of the oxygen produced by the electrolysis cells improves significantly the environmental performance of the proposed process.

1. Introduction

The largest source of greenhouse gas emissions from human activities in the world is from burning fossil fuels for electricity and heat, contributing to over half of the total CO_2 emissions in the atmosphere [1]. The recent spread of renewable energy technologies, such as onshore and offshore wind and solar photovoltaic, is a symptom of a new responsiveness to environmental issues by the energy sector. In the last decade, only in the European Union electricity production from renewable sources increased nearly fourfold, from 127 to 476 TWh per year [2]. However, the integration of large amounts of renewable energies into the existing energy grid poses significant technological difficulties that are consequence of the intrinsic variability of renewable sources [3]. Therefore, the ability to store effectively excess of electrical

energy from peaks of production is key to the development and the deployment of renewable energies.

Power-to-Gas (PtG) technologies represent the most promising option for the provision of large-scale, flexible energy storage by converting electrical into chemical energy [4]. Hydrogen, which is usually the product of this conversion, can be used as a fuel or injected into the natural gas network (up to a limit volumetric percentage), but for long-term storage it is usually recommended conversion of hydrogen to more stable fuels and/or chemicals [3]. Methane represents an attractive possibility because it enables to store large amounts of energy from renewable sources for long time scales in an already existing storage system: the natural gas grid; and because it can be directly used in most of endothermic engines and all other well-established natural gas facilities. Power-to-Methane (PtM) is a two-step process that involves the production of hydrogen, typically by electrolysis of water, and its

---

Nomenclature

Latin Letters

A_k	Total number of atomic masses,
a	Stoichiometric coefficient,
c_p	Specific heat, J/(kg·K)
D	Diameter, m
$\widehat{f}_i$	Fugacity of species i, bar
f_i°	Fugacity of species i at standard state, bar
G_i	Gibbs free energy of species i in the gas mixture, J
G_i°	Gibbs free energy of species i at its standard state, J
G_{if}°	Gibbs free energy of formation for species i at standard state, J
h	Height of the solids bed, m
K	Constant, m s
m	Mass, kg
$\dot{n}$	Molar flow rate, mol/s
P	Pressure, bar
$\dot{Q}$	Thermal power, W/s
Q	Specific volumetric flow rate, Nm^3/kg
r	Reaction rate, mol/s
R	Constant, J/(mol K)
S	Entropy, J/K
T	Temperature, K
t	Time, s
U	Superficial gas velocity, m/s
W	Solids mass flow rate, kg/s

Greek Letters

α	Constant, m^{-1} s^{-1}
ΔH_r	Standard enthalpy, J
δ	Bubble fraction,
ε	Voidage fraction,
$\nu_{i,k}$	Number of atoms,
ρ	Density, kg/m^3
η_{ec}	Electric energy conversion efficiency,

Acronyms

AEL	Alkaline Electrolysis
AR	Air reactor
CLC	Chemical Looping Combustion
CLOU	Chemical Looping with Oxygen Uncoupling
EF	Environmental footprint
FR	Fuel reactor
HP-PEM	High-Pressure Polymer Electrolyte Membrane cells
JRC	Joint Research Centre
LCA	Life Cycle Assessment
MFB	Multiple interconnected Fluidized Beds
MR	Methanation reactor
OC	Oxygen Carrier
PEM	Polymer Electrolyte Membrane
PtG	Power to Gas
PtM	Power to Methane
SOEC	Solid Oxide Electrolysis Cell
t-FR	Two stage Fuel Reactor

Subscript and superscript

B	Bed
BB	Bottom bed
in	Inlet flow
LS	Loop seal
LV	L-valve
mf	Minimum fluidization
oc	Oxygen carrier
out	Outlet flow
p	Particle
R	Riser
S	Solids
SBB	Solid bottom bed
slug	Slug
STB	Solid top bed
TB	Top bed
TR	Transfer riser

conversion to methane using either CO or CO_2 as a source of carbon. Thus, the process can also represent a mean to mitigate carbon emissions from large fixed sources.

Absorption of carbon dioxide into liquid solvents such as alkanolamines is most widely used carbon capture technology in industrial processes (e.g. ammonia production), primarily thanks to a good compromise between the rate of CO_2 capture and the cost of solvent regeneration through CO_2 desorption [5]. However, research is still active in the selection of alternatives to reduce both pollutant emissions and CO_2 capture stage costs, which accounts for up to 80% of operating costs [4]. Chemical-looping systems are under the spotlight as more efficient and cost-effective technologies than commercially available ones. Chemical Looping is based on the cyclic exposition of a solid metal oxide – known as oxygen carrier (OC) - to two different reactive environments (i.e. two different reactors connected in a loop or two different streams alternatively fed to the same reactor), which enables selective transport of a chemical, such as oxygen or carbon dioxide, between otherwise uncoupled devices/environments [6]. Among Chemical Looping systems, Chemical Looping combustion with Oxygen Uncoupling (CLOU) is a very promising technology for solid fuels combustion with inherent CO_2 sequestration.

The CLOU concept is based on two cyclic steps: in the first one, the oxygen carrier is reduced releasing gaseous oxygen for fuel oxidation, whilst in the second step the reduced oxygen carrier is re-oxidized by air. Therefore, direct contact between the fuel and the atmospheric oxygen is avoided, and flue gases are mainly composed of CO_2 and H_2O, with the latter being easily separated by condensation. The two steps occur in two reactors (named Fuel Reactor and Air Reactor) typically arranged in a dual interconnected fluidized bed configuration. This arrangement enables recirculation of the oxygen carrier between the reactors and ensures good contact between the gaseous and solid phases. However, this arrangement also presents some criticalities that are related to the effective control of solids recirculation and to the establishment of leak-tight operation of the beds with respect to the gaseous streams; these can be mitigated by correctly selecting both design and operational variables of the plant [7] and, with respect to a successful CLC of solid fuels, by properly selecting the OC and a correct design of the fuel reactor. Oxygen carriers suitable for CLOU should obviously be able to release gaseous oxygen and this O_2 release must be reversible. Therefore, only metal oxides having a proper equilibrium partial pressure of oxygen at CLOU typical operating temperatures (800–1200 °C) can be used. According to Ref. [8], such metal oxide systems are generally composed of an active phase consisting of metal oxides of the transition group (CuO/Cu_2O, Mn_2O_3/Mn_3O_4, and Co_3O_4/CoO) coupled with a support, usually alumina or zirconia. Among them, the one most suitable for the proposed application (*i.e.* the one with the highest oxygen transport capacity under the CLC operating conditions) is the CuO/Cu_2O [9].

As mentioned above, in PtM systems hydrogen is produced by electrolysis of water using the excess electrical energy. Three different electrolysis technologies are suitable to PtG: alkaline electrolysis (AEL),
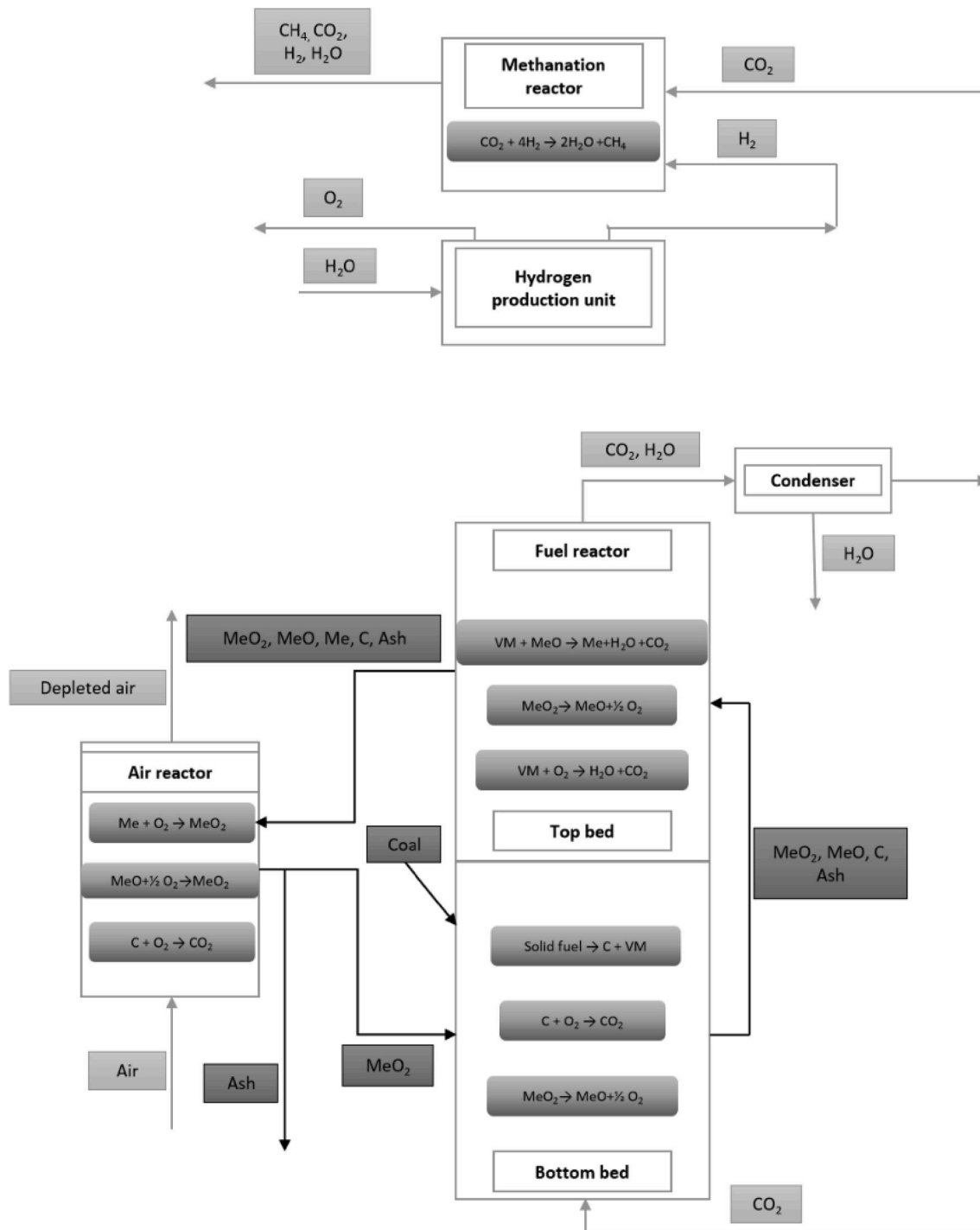
Fig. 1. Conceptual scheme of the proposed process.

polymer electrolyte membranes (PEM), and solid oxide electrolysis (SOEC). AEL represent a mature technology that has low installation costs and a reasonable lifetime, and that is available for large plant sizes. However, the technology has high maintenance costs (due to the system being highly corrosive), and during transient operation the nominal load can decrease by as much as 20%. Recently PEM has been emerging as an alternative to AEL because i) it does not require corrosive substances, ii) it can reach high power densities and high operating pressure (>100 bar), and iii) it can be operated dynamically. However, PEM has high installation costs and degrades fast. SOEC represents a very promising electrolysis technology but has only been tested at laboratory scale.

Finally, in the second step of PtM, H_2 and CO_2 are converted into methane. Several methanation reactor designs have been proposed and investigated in the literature [10], ranging from multiple adiabatic layers fixed beds to fluidized bed reactors, in order to control the temperature rise associated to the highly exothermic Sabatier reaction so to avoid catalyst sintering while approaching the best thermodynamic condition for the process.

In this work, we propose an innovative process layout that integrates two-stage Chemical Looping Combustion of solid fuels with Oxygen Uncoupling, hydrogen production through water electrolysis by PEM, and methanation. To the best of the authors' knowledge, there is no previous work in the literature proposing the same configuration. We investigate both the technical and environmental performance of the
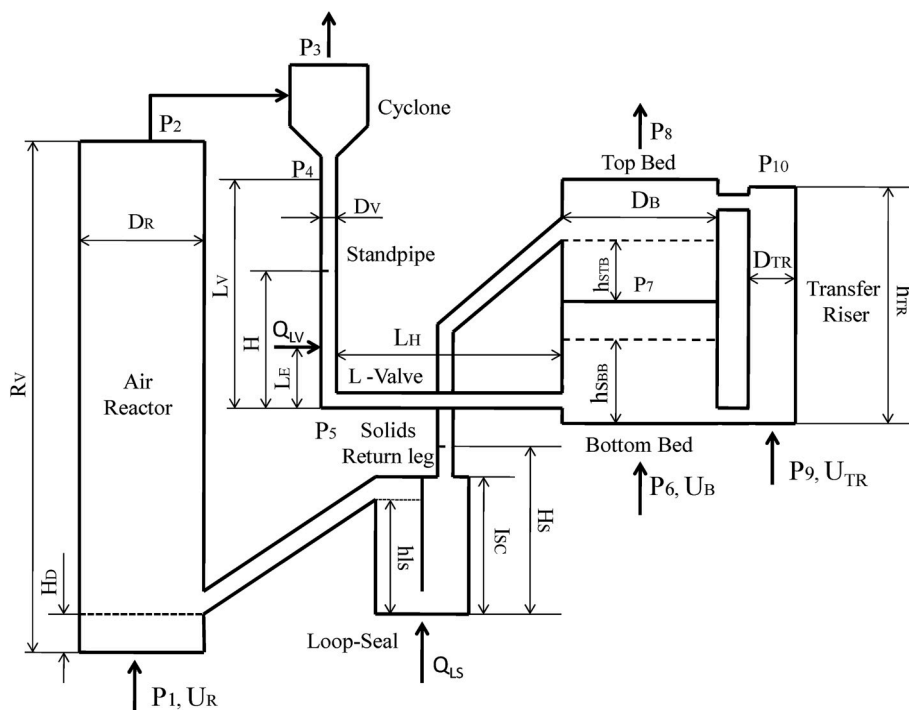
Fig. 2. Schematic representation of the MFB system along with the indication of main geometric and operating variables.

system, with specific reference to the Italian context where vast amounts of electricity from renewable sources are wasted (i.e. not dispatched nor stored [11]) as a consequence of the intrinsic structure of the Italian transmission grid. The technical performance is assessed in terms of the thermal power generated by MFB-CLOU and methanation units, the number of electrolysis cells required to produce hydrogen, the CH_4 flow rate, and the energy conversion efficiency. The environmental performance is evaluated using the Life Cycle Assessment methodology. LCA is a widely used methodology for quantifying the environmental impacts associated with products and services [12,13]. The holistic perspective represents the key feature of LCA: the methodology considers the whole life cycle of a product/service, from the extraction of raw materials to the management and disposal of end-of-life wastes.

2. Mathematical model

2.1. Hydrodynamic and kinetic model

Fig. 1 reports the conceptual scheme of the proposed layout with details on reactive pathways, and outlet and inlet material streams.

The core of the layout consists of a multiple interconnected fluidized bed system equipped with a two-stage fuel reactor, a riser used as Air Reactor, a cyclone, a L-valve return leg, and a loop-seal, as sketched in Fig. 2.

The t-FR is based on the concept presented in a previous work [14], where two bubbling beds were placed in series with respect to both gaseous and solids streams in order to overcome the limitations of a single-stage FR. The first stage is mainly devoted to the combustion of the char exploiting oxygen release from the fully oxidized oxygen carrier (CLOU effect), while in the second stage the conversion of the volatile matter by the residual oxidative potential of the oxygen carrier took place. An internal riser connects the two stages, thus allowing the solids to move from the first stage to the other. Solids from the second stage go through the loop-seal into the AR where the oxidation capability of the OC is restored. A cyclone collects the regenerated OC that is sent through the L-valve to the first stage of the t-FR. At the exit of the second stage, water and fines were separated from flue gas. This latter is partly

conveyed to a methanation unit in order to react with a hydrogen stream coming from an electrolysis cells array, while the remnant is recycled to the t-FR.

The hydrodynamics of the MFB-CLC has been modelled as a combination of mutually interconnected blocks: risers, valves, downcomers, and a cyclone. For each block, material and momentum balance equations were written after selection of proper constitutive equations, neglecting the contribution of coal, char and ash particles to the hydrodynamics of the various components of the system. For the sake of brevity, only equations added with respect to our previous work are reported here. More details on hydrodynamic model can be found in the Supporting Information.

With respect to the t-FR, a simplified formulation of the momentum equation has been considered. It assumes that the gas pressure drop across the beds is only due to the contribution of the gravitational forces, according to:

$$P_6 - P_7 = (1 - \varepsilon_B)\rho_p g h_{SBB} + \rho_g g(h_{BB} - h_{SBB}) \tag{1}$$

$$P_7 - P_8 = (1 - \varepsilon_B)\rho_p g h_{STB} + \rho_g g(h_{TB} - h_{STB}) \tag{2}$$

where P_6, P_7, P_8, ρ_p, ε_B, h_{SBB}, h_{STB}, h_{BB}, and h_{TB} are the pressures at the inlet and at the exit of the bottom and the top beds, the particle density, the bed voidage, the heights of the solids in the bottom and in the top bed and of the bottom and the top bed themselves, respectively. Under the assumption that elutriation is negligible, the solid mass flow rate at the outlet of t-FR is equal to that supplied from the L-valve, if the height of solid reaches the weir that connects the top bed to the loop-seal, otherwise it is zero.

The transfer riser operates in slug conditions and consequently the pressure drop along it depends both on the contribution due to the gravitational force and on the wall friction of solids flowing along the riser. Accordingly, it could be written as:

$$P_9 - P_{10} = \rho_P(1 - \varepsilon_B)g h_{TR} + \alpha W_{B1} \tag{3}$$

where P_9, P_{10}, h_{TR}, α, and W_{B1} are the pressures at the bottom and at the exit of the transfer riser and its height, a proportionality constant and the

solid mass flow rate at the outlet of the transfer riser itself and ρ_r is the mean density along the transfer riser, evaluated as:

$$\rho_r = \rho_{mf}(1 - \delta) \tag{4}$$

where:

$$\delta = \frac{U_{TR} - U_{mf}}{U_{TR} - U_{mf} + U_{slug}} \tag{5}$$

U_{TR}, U_{mf}, U_{slug} are the gas superficial velocity in the transfer riser, the minimum fluidization velocity, and the slug velocity, respectively. This latter, according to Ref. [7], could be expressed as:

$$U_{slug} = 0.35\sqrt{gD_{TR}} \tag{6}$$

where D_{TR} is the transfer riser diameter. The solid mass flow rate in the transfer riser is proportional to the pressure drop P_9–P_6; accordingly, it could be written that:

$$W_{B1} = K(P_9 - P_6) \tag{7}$$

Substituting (1)–(3) in (7) and considering that $P_8 = P_{10} = P_{atm}$, the latter equation can be rearranged as:

$$W_{B1} = \frac{K}{1 + \alpha K} g\rho_{mf}(\delta h_{TR} - h_{TR} + h_{SBB} + h_{STB}) \tag{8}$$

In order to make the system well-conditioned, the following global momentum and mass balances equation was written:

$$\begin{cases} (P_3 - P_4) + (P_4 - P_5) + (P_5 - P_6) + (P_6 - P_7) + (P_7 - P_8) = 0 \\ (P_7 - P_8) + (P_7 - P_6) + (P_6 - P_9) + (P_9 - P_{10}) = 0 \\ (P_8 - P_1) + (P_1 - P_2) = 0 \\ m_{inv} = m_R + m_{LV} + m_{BB} + m_{TB} + m_{TR} + m_{LS} \end{cases} \tag{9}$$
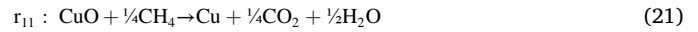
where m_{inv}, m_R, m_{LV}, m_{BB}, m_{TB}, m_{TR}, and m_{LS} are the solid inventory, the mass of solids in the riser, in the L-valve, in the bottom and in the top beds, in the transfer riser, and in the loop-seal, respectively.

The transient behaviour of the system was modelled by considering the following set of ODEs and associated initial conditions:

$$\begin{cases} \dfrac{dm_{LV}}{dt} = W_R - W_S; \ m_{LV}(0) = m_{LV0} \\[2mm] \dfrac{dm_R}{dt} = W_{LS} - W_R; \ m_R(0) = m_{R0} \\[2mm] \dfrac{dm_{LS}}{dt} = W_{B2} - W_{LS}; \ m_{LS}(0) = m_{LS0} \\[2mm] \dfrac{dm_{BB}}{dt} = W_S - W_{B1}; \ m_{BB}(0) = m_{BB0} \\[2mm] \dfrac{dm_{TR}}{dt} = W_{B1} - W_{B2}; \ m_{TR}(0) = m_{TR0} \end{cases} \tag{10}$$

A coupled hydrodynamic and kinetic model of the MFB is applied in order to evaluate flue gas composition and flow rate, and power production. A combination of mutually interconnected blocks (risers, valves, downcomers, and a cyclone) was used to represent the unit.

The gas-solid heterogeneous reactions taking place in the fluidized beds and the gas-phase homogeneous reactions occurring in the freeboard of fuel reactors implemented in the model were:

$$r_1: \ C + CO_2 \rightarrow 2CO \tag{11}$$

$$r_2: \ CuO + \tfrac{1}{2}CO \rightarrow \tfrac{1}{2}Cu_2O + \tfrac{1}{2}CO_2 \tag{12}$$

$$r_3: \ Cu_2O + CO \rightarrow 2Cu + CO_2 \tag{13}$$

$$r_4: \ CuO \rightarrow \tfrac{1}{2}Cu_2O + \tfrac{1}{4}O_2 \tag{14}$$

$$r_5: \ CO + \tfrac{1}{2}O_2 \rightarrow CO_2 \tag{15}$$

$$r_6: \ C + O_2 \rightarrow CO_2 \tag{16}$$

$$r_7: \ C + H_2O \rightarrow CO + H_2 \tag{17}$$

$$r_8: \ H_2 + \tfrac{1}{2}O_2 \rightarrow H_2O \tag{18}$$

$$r_9: \ CuO + \tfrac{1}{2}H_2 \rightarrow \tfrac{1}{2}Cu_2O + \tfrac{1}{2}H_2O \tag{19}$$

$$r_{10}: \ Cu_2O + H_2 \rightarrow 2Cu + H_2O \tag{20}$$

$$r_{11}: \ CuO + \tfrac{1}{4}CH_4 \rightarrow Cu + \tfrac{1}{4}CO_2 + \tfrac{1}{2}H_2O \tag{21}$$

$$r_{12}: \ CH_4 + 2O_2 \rightarrow CO_2 + 2H_2O \tag{22}$$

$$r_{13}: \ 2Cu + O_2 \rightarrow 2CuO \tag{23}$$

$$r_{14}: \ Cu_2O + \tfrac{1}{2}O_2 \rightarrow 2CuO \tag{24}$$

Reactions 11–22 were considered to occur in the fuel reactor, whereas reactions 16, 23 and 24 apply to the air reactor. The whole set of heterogeneous and homogeneous reactions could be classified into three different categories: reactions involving carbon (11, 16, 17), reactions involving the oxygen carrier (12–14, 19–21, 23, 24), and reactions of the volatiles (15, 18, 22). More details on the adopted reaction kinetics can be found in Supporting Information.

Model equations consist of mass and energy balances on reagents and products. Mass balance equations, specialized to model the dense phase for both the bottom and the top bed, were referred or to single elements (i.e. C, H, O, Cu) or to specific compounds (i.e. CO_2, char, CH_4, H_2O) assuming the following general form:

$$\sum \dot{n}_i^{in} - \sum \dot{n}_i^{out} + \sum (a_{i,j} \cdot r_j) = 0\overline{Y} \tag{25}$$

where $\dot{n}_i^{in}$ and $\dot{n}_i^{out}$ represent respectively the ith species inlet and the outlet molar flow rate and r_j denotes the kinetic term of the jth reaction involving the ith species by the stoichiometric coefficient $a_{i,j}$.

Energy balance equations, used to calculate the thermal power at the chosen operating temperature, were expressed as:

$$\dot{Q} = \sum \dot{n}_i^{in} \cdot c_{p,\ i} \cdot (T^0 - T_i^{in}) + \sum \dot{n}_i^{out} \cdot c_{p,\ i} \cdot (T_i^{out} - T^0) + \sum \left(-\Delta H_{r_j}^0\right) \cdot r_j \tag{26}$$

where $c_{p,\ i}$ is the specific heat capacity and $\Delta H_{r_j}^0$ is the standard enthalpy of reaction of the ith species, while is the thermal power. The specialized set of equations for each chemical species is reported in Supporting Information.

Given proximate and ultimate analysis of the fuel, operating pressure and temperature of both the Fuel and Air reactors, the outputs of the mathematical model are the total thermal power ($P_{,T,Th}$) - negative if generated and positive if required - to carry out isothermally the CLC, the composition and flow rate of flue gas, the required oxygen carrier mass flow rate (m_{oc}), and the fluidizing gas flow rate to the Air reactor (m_{air}).

The methanation reactor (MR) has been modelled considering that CO_2 reacts with H_2 over Ni supported on alumina catalyst under equilibrium conditions and developing a thermodynamic calculation method based on the minimization of the free Gibbs energy. Such a method does not rely on the actual reactor type, thus greatly reducing the computational effort, and is based on the principle that the system total Gibbs energy, accounting for condensed and non-reacting species too, reaches its minimum value at chemical equilibrium. Accordingly, if all the species, both reactants and products, in a reactive system are known, the concentration values at equilibrium can be evaluated by using a general mathematical technique even if the kinetic pathway is unknown. In the case of methanation processes, although reactions pathway is well known (see, for instance Ref. [15]), the mathematical problem of finding the equilibrium composition can be reformulated as the search for the minimum of the total Gibbs energy, neglecting the kinetic description of

the process. The total Gibbs energy is given by:

$$(G^t)_{T,P} = g(n_1, n_2, n_3, \ldots, n_N) = \sum_{i=1}^{N} n_i G_i^\circ + RT \sum_{i=1}^{N} ln\left(\frac{\widehat{f_i}}{f_i^0}\right) \tag{27}$$

The problem is to find the set n_i which minimizes G^t for given values of pressure and temperature, subject to the constraints of the material balances. The material balance on each element k may be written assuming that the total number of atoms of each element is constant:

$$\sum_i n_i v_{i,k} = A_k \tag{28}$$

In Eq. (28) A_k is the total number of atomic masses of the kth element (C, H, O) in the system, as determined by the initial constitution of the system; $v_{i,k}$ is the number of atoms of the kth element present in each molecule of chemical species i. The Gibbs energy for these species is calculated from the Gibbs-Helmholtz relation:

$$G = H - TS \tag{29}$$

where:

$$H = H_{298} + \int_{298}^{T} C_P dt$$
$$S = S_{298} + \int_{298}^{T} \frac{C_P}{T} dt \tag{30}$$

The enthalpy at 298 K, H_{298}, is set to zero by convention. The entropy, S_{298}, is given by its absolute value, and the heat capacity at constant pressure, c_p, is calculated as:

$$c_p = A + B \cdot T + C \cdot T^2 + D \cdot T^3 + \frac{E}{T^2} \tag{31}$$

The coefficients of Eq. (21) are from NIST Chemistry WebBook [16]. For solid Carbon a simplified formula for c_p has been used [17]:

$$c_p = A + B \cdot T - \frac{C}{T^2} \tag{32}$$

The hydrogen production unit was modelled as an array of high-pressure polymer electrolyte membrane cells (HP-PEM). The number of HP-PEMs to be arranged in the array was evaluated by considering that a constant hydrogen production able to stoichiometrically convert the whole CO_2 stream produced by the CLC process should be attained.

Finally, the electric energy conversion efficiency (η_{ec}), defined as the ratio between the electric energy output and input of the system, was evaluated to assess the capability of the proposed process to be used as an energy storage system, according to:

$$\eta_{ec} = \frac{Q_{CH_4} \cdot LHV_{CH_4} \cdot CF \cdot \eta_e}{Electric\ energy\ input} \tag{33}$$

where Q_{CH_4} is methane volumetric flow rate, LHV_{CH4} is methane low heating value, CF is the capacity factor, *i.e.* the annual number of running hours, and η_e is thermal-to-electric conversion efficiency.

2.2. Operating conditions

The hydrodynamic model was solved using the commercial software package COMSOL Multiphysics®. Properties of fluidization gas, bed material, key geometrical features of the components, and operating conditions of both t-FR and AR were reported in the Supporting Information, with the exception of the transfer riser height and diameter (1.93 m and 0.04 m, respectively), t-FR diameter (0.38 m), and top- and bottom-bed height (1 m).

Properties of solid fuel, evaluated by means of proximate and ultimate analysis, carried out by LECO CHN 628, LECO CS 144 and LECO TG701, are reported in Table 1.

Table 1
Properties of considered fuel.

Proximate analysis, -	
Moisture	0.1
Volatiles	0.2
Fixed carbon	0.6
Ash	0.1
Ultimate analysis, -	
C	0.7
H	0.1
N	0.0
S	0.1
O	0.1

For the MFB-CLC unit, operating pressure was set at 10^5 Pa while fuel and air reactor operating temperatures were set at 1173.15 K and 923.15 K, respectively.

For the methanation unit, operating pressure was varied between 1 and 50 bar while temperature was varied between 558.15 K and 1100 K, the former being the activation temperature of the chosen catalyst. Under the above operating conditions, ideal gas state equation can be safely considered in the evaluation of Eq. (27); accordingly, $\widehat{f}_i = P y_i$, $f_i^\circ = 1$, and $G_i^\circ = \Delta G_{i,f}^\circ$.

For the evaluation of the number of HP-PEMs to be arranged in the array, data from commercially available units were considered [18]. Accordingly, a nominal H_2 production flowrate of 100 Nm³/h and an electric energy efficiency equal to 46.6 kWh/kg$_{H2}$ were taken into account. It should be noted here that, according to Ref. [2,11], around 360 GWh of wind-produced electric energy were wasted (not dispatched nor stored) in Italy over the last 3 years as a consequence of the zonal structure of the Italian transmission grid that tends to cap energy flows from southern regions (where it is mainly produced) to northern ones (where most of energy consuming factories are). Due to the magnitude of this wasted electricity, it is reasonable to assume that the HP-PEMs array operates in continuous.

2.3. Life Cycle Assessment

The Life Cycle Assessment methodology is deployed to identify the main sources of environmental impacts (i.e. "hot-spots") associated with the innovative layout introduced above and to assess its environmental performance compared with an equivalent system of reference that delivers the same functions. The analysis is specific to the Italian context (see Section 1); this means that, where available, inventory data specific to Italy is used.

The proposed system has the twofold function of generating electricity and producing methane. Notably, we assume a 30% efficiency in converting the thermal energy generated by the Chemical Looping Combustion (CLC) reactor to electricity. We also assume that wasted electricity from onshore wind farms is used to produce hydrogen from water. The reference system for comparative purposes comprises the conventional pathways to generate electricity and to produce methane: electricity is assumed to be generated according to the Italian electricity grid mix, whilst methane is produced from conversion of natural gas. The functional unit, which in LCA represents a quantified description of the functions delivered by the system, is equal to 1 kWh of electricity generated and 0.49 kg of methane produced. Fig. 3 illustrates the comparative analysis performed. The system boundary of the proposed innovative layout is divided into Foreground and Background [19]. The former is defined as the "processes whose selection or mode of operation is affected directly by decisions based on the study" [19], and includes the CLC, the high-pressure polymer electrolyte membrane (HP-PEM) and methanation units. The latter includes all other processes which interact with the foreground; notably, Fig. 3 reports as "black boxes" the processes of production, transportation and disposal of oxygen carrier
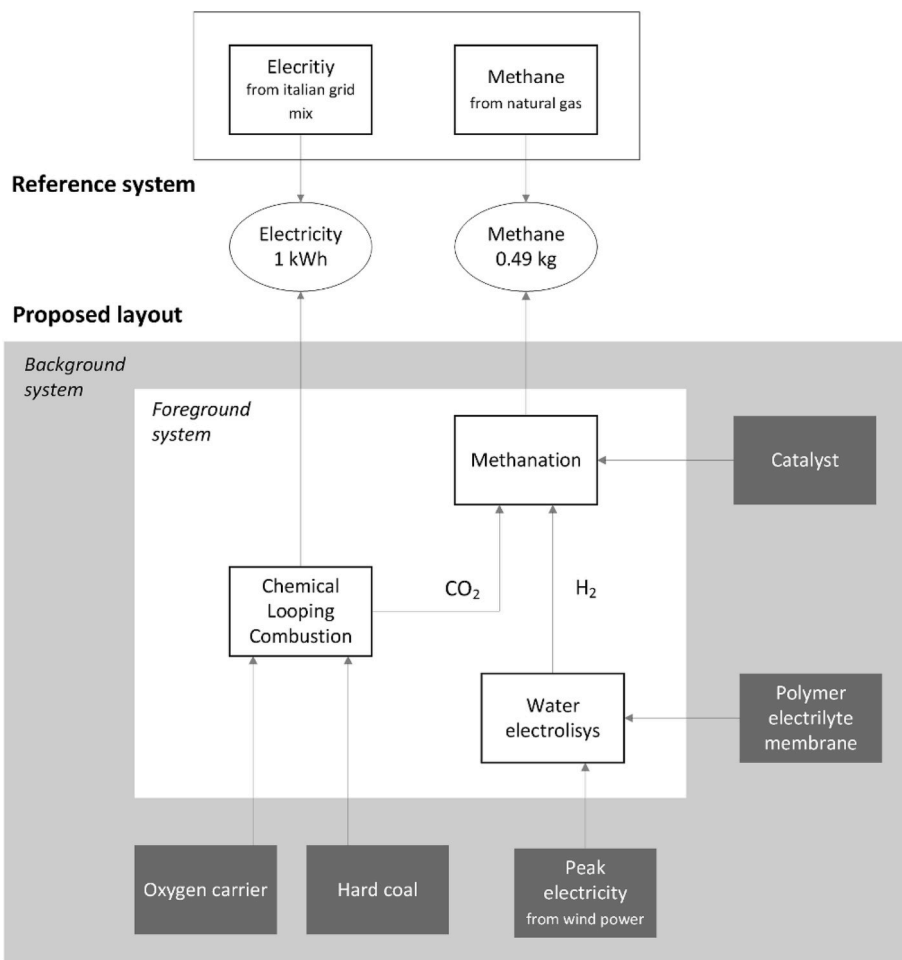
Fig. 3. Simplified boundaries of the comparative analysis between the innovative process proposed in this study and the reference system. For simplicity, the diagram does not include the construction phase of the units in the Foreground system.

and hard coal used by the CLC unit, polymer electrolyte membrane for the HP-PEM unit and nickel catalyst for the methanator, and the processes of generation and distribution of electricity from wind power. The construction phase is not reported explicitly in Fig. 3 but is considered for all units in the Foreground and Background system. The study does not include decommissioning of the facilities in the Foreground system. For the reference system Fig. 3 only reports the two processes of reference for methane and electricity production, which includes all activities in their life-cycle.

The life-cycle inventory is based on the results of the mathematical model developed in this study and on literature data, and is reported in the Supporting Information. Results of the model presented in this study (Sections 2.1 and 2.2) are used to describe the operation of the CLC reactor and of the methanation unit in terms of mass and energy inputs/outputs. Data for the HP-PEM unit is based on this study and on the Ecoinvent database, version 3.5 cut-off model [20]. Data on the construction phase is obtained from Ecoinvent for the CLC reactor (note that we assume that construction of the CLC reactor for electricity production is equivalent to that of a coal power plant), on Ecoinvent and [18] for the HP-PEM cell, and on [21,22] for the methanation reactor using a nickel catalyst. The oxygen carrier is assumed to consists of 50% copper oxide and 50% zirconia; data on its production is on a laboratory scale and is based on [23]. Finally, life-cycle inventory data for the remaining activities in the Background system, and for the conventional pathway to methane production and electricity from the Italian grid mix (which primarily comprises of 28% natural gas, 15% coal, 22% hydro, 6% wind and 17% imported from other countries) are obtained from the

Table 2
Environmental impact categories analysed.

IMPACT CATEGORY	METRIC
Acidification	Mole of H+ eq.
Cancer human health effects	CTUh
Climate change	kg CO2 eq.
Ecotoxicity freshwater	CTUe
Eutrophication freshwater	kg P eq.
Eutrophication terrestrial	Mole of N eq.
Ionizing radiations	kBq U235 eq.
Non-cancer human health effects	CTUh
Photochemical ozone formation - human health	kg NMVOC eq.
Resource use, energy carriers	MJ
Resource use, mineral and metals	kg Sb eq.
Respiratory inorganics	Deaths

Ecoinvent database.

The Environmental Footprint (EF) 2.0 method developed by the Joint Research Centre (JRC) of the European Commission [24,25] is used for quantifying the environmental impacts. We included all impact categories, but report climate change impacts only in terms of the sum of the contributions from fossil and biogenic greenhouse gases and land-use change. A description of these environmental impact categories can be found at [26]. For the comparative analysis, the environmental impacts are normalized to the reference impact per person of EU-28 using the EF 2.0 normalization factors [27].

In the article we focus on 12 impact categories, reported in Table 2, which feature normalized impacts higher than an arbitrarily set

Table 3
MFB-CLC model outputs.

$P_{,T,Th}$, kW/s	4.3
Q_{CO2}, Nm^3/s	$3.7\ 10^{-4}$
m_{oc}, kg/s	$1.0\ 10^{-2}$
Q_{air}, Nm^3/s	$3.7\ 10^{-6}$

Table 4
HP-PEM model outputs.

N_c, -	$5.3\ 10^{-2}$
Q_{H2}, Nm^3/s	$1.5\ 10^{-3}$
Q_{O2}, Nm^3/s	$7.4\ 10^{-4}$

threshold of 10^{-4} persons equivalent for both the proposed layout and the reference system.

3. Results and discussion

3.1. Technical performance

Table 3 reports, with respect to 1 kg/h of fuel fed, the generated thermal power ($P_{,T,Th}$), the CO_2 volumetric flow rate (Q_{CO2}), the required oxygen carrier mass flow rate, and the fluidizing gas flow rate to the Air reactor.

The required H_2:CO_2 ratio for the methane synthesis is 4:1 [8]. On the basis of the CO_2 volumetric flow rate at the exit of the fuel reactor (Table 3), the hydrogen (Q_{H2}) and oxygen (Q_{O2}) volumetric flow rates and the number of electrolytic cells (Nc) can be consequently evaluated. Data are reported in Table 4.

Fig. 4 reports, as a function of the operating temperature, the gas molar fractions at the output of the methanation unit parametric with the operating pressure. The analysis of the above figure suggests that, whatever the operating pressure, in order to achieve high methane content operating temperature should be set as low as possible. A low operating temperature has furthermore the beneficial effects to avoid carbon monoxide formation and to keep hydrogen concentration as low as possible.

In principle, depending on type of catalyst, feed gas composition, and operating conditions, it should be noted that carbon deposition on supported catalyst can occur (according to the Boudouard reaction); in order to avoid this, temperature should be kept high or CO_2 and/or H_2O has to be added to the feed (e.g. Ref. [28]).

However, under the current assumption that H_2 and CO_2 are stoichiometrically fed to the methanation unit, no carbon deposition can occur. Accordingly, it could be settled that, above catalyst activation temperature, the lower the operating temperature the better in terms of methane concentration, notwithstanding the operating pressure.

With respect to the choice of the optimal operating pressure, an analysis of the same figure suggests that, for any given operating temperature, increasing the methanation unit pressure from 5 to 20 bar significantly increases both methane and water molar fraction while reduces residual hydrogen content. However, an increase in operating pressure from 20 to 50 bar does not alter appreciably gas composition as long as the operating temperature is close to catalyst activation one.

Altogether, it can be inferred that: i) with respect to the choice of the operating temperature, above catalyst activation temperature the lower, the better; ii) with respect to the choice of the operating pressure, a "threshold" pressure value exists for any given temperature beyond which any further pressure increase does not correspond to substantial variations in both hydrogen and methane concentrations.

From the above cited figure, it can additionally be seen that water concentration is always higher than methane one, so drying of the methanation output stream is mandatory. After water removal, the concentration of methane boosts together with the residual concentrations of both hydrogen and carbon dioxide. In order to improve process methane yield, a second methanation unit is therefore considered in series with the first one. Table 5 reports the carbon dioxide (Q_{CO2}), hydrogen, and methane (Q_{CH4}) volumetric flow rates at the output of

Table 5
Methanation units model outputs.

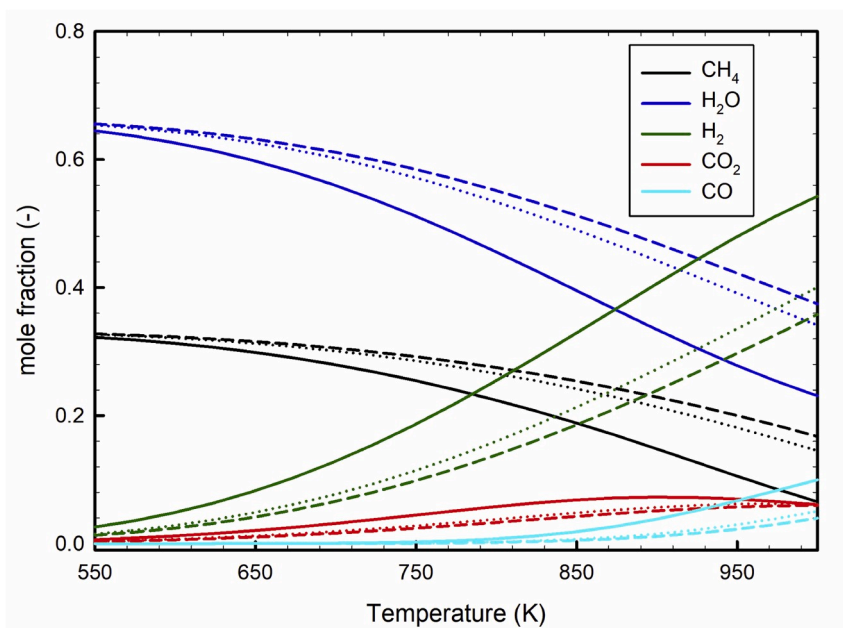| T, K	558	623
$Q_{CO2}\ 10^8$, Nm^3/kg	7.4	9.8
$Q_{H2}\ 10^6$, Nm^3/kg	7.0	9.8
$Q_{CH4}\ 10^4$, Nm^3/kg	3.3	3.3

Fig. 4. Gas molar fractions at the outlet of methanation unit as a function of the operating temperature at an operating pressure of 5 bar (solid lines), 20 bar (dotted lines), and 30 bar (dashed lines).
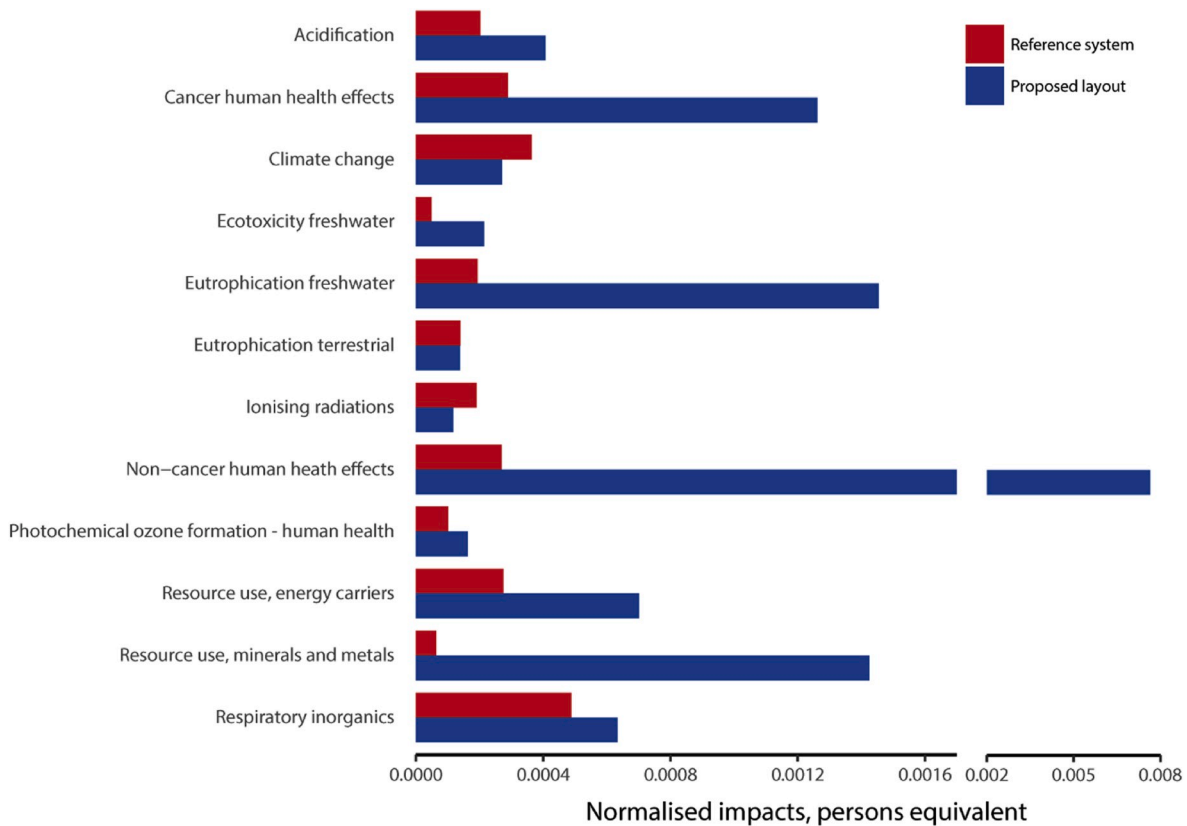
Fig. 5. Comparison between normalized environmental impacts of the proposed process layout and the reference system.

this second unit when the operating pressure is set at 20 bar and the operating temperature varies in a narrow interval above the catalyst activation one. An almost complete conversion of CO_2 and H_2 is obtained, whatever the operating temperature considered. More specifically, the conversion degrees are 99.2% and 98.5% for 558 and 623 K, respectively. With respect to methane concentration, in both cases a value higher than the required one for its injection into the natural gas grid (*i.e.* > 95%) is achieved.

The electric energy conversion efficiency evaluated for the proposed process is ~16%, regardless of the methanation unit operating temperature and pressure.

3.2. Environmental performance

Numerical results of the LCA study are included in the Supporting Information. Fig. 5 reports the comparative analysis in terms of normalized impacts between the proposed layout and the reference systems.

The chart shows that the proposed process outperforms the reference system only with respect to the categories climate change and ionizing radiations, whilst it has a similar performance in the category terrestrial eutrophication. Specifically, the proposed layout delivers a reduction of about 25% of impacts due to greenhouse gases, and about 40% of impacts on humans due to radionuclides. However, the proposed process yields significant increases in other impact categories, as high as ~28 times for non-cancer human health effects and ~22 times for the depletion of minerals and metals; the impact in both categories is attributable to oxygen carrier, specifically to its disposal for the former and to its production for the latter as explained below. The normalization procedure also reveals that carcinogenic and non-carcinogenic toxic impacts (which originate from activities in the background system), freshwater eutrophication and depletion of mineral and metals represent the most critical impact categories for the proposed process.

Fig. 6 reports the hot-spot analysis for the process developed in this article. It is evident from the chart that the largest portion of the environmental impacts originate from the CLC unit, with contributions ranging from 90% in the category "ionizing radiations" and up to ~100% in the category "freshwater eutrophication".

Interestingly, the results from the LCA analysis reveal that the impacts of the CLC unit are primarily attributable to the production of the oxygen carrier (OC), and, for carcinogenic and non-carcinogenic human health impacts, to its disposal (see Fig. S2 in the Supporting Information). Similar results are found by Ref. [23]. The amount of OC used up by the CLC reactor includes an initial loading plus additional amounts to make up for the loss of the carrier due to elutriation (~0.5% of the OC mass flow rate within the CLC unit); the OC lost by elutriation is assumed to be captured by filters and treated as hazardous waste, which, according to Ecoinvent, entails incineration and landfilling. The environmental impacts associated with the production of the oxygen carrier are approximately equally shared between production of copper oxide and zirconium oxide with the exception of the category climate change, where energy consumption represent the dominant source of impacts.

The proposed layout represents therefore a valid solution only with respect to climate change and ionizing radiations impacts; the performance in the remaining categories is poor when compared to the conventional technologies. The results of the LCA analysis suggest that efforts to improve its environmental performance should be primarily focused on the oxygen carrier.

An effective strategy could be to reduce the amount of oxygen carrier used by the CLC system by directly feeding part or all of the oxygen produced in the HP-PEM unit to the t-FR unit. This in fact reduces the amount of both the OC needed to carry out CLC (since part of the fuel directly reacts with gaseous oxygen) and the spent OC to be treated. Under the current assumption that the amount of hydrogen produced in the HP-PEM units is that needed to stoichiometrically convert the whole CO_2 stream fed to the methanation unit, double the oxygen required to
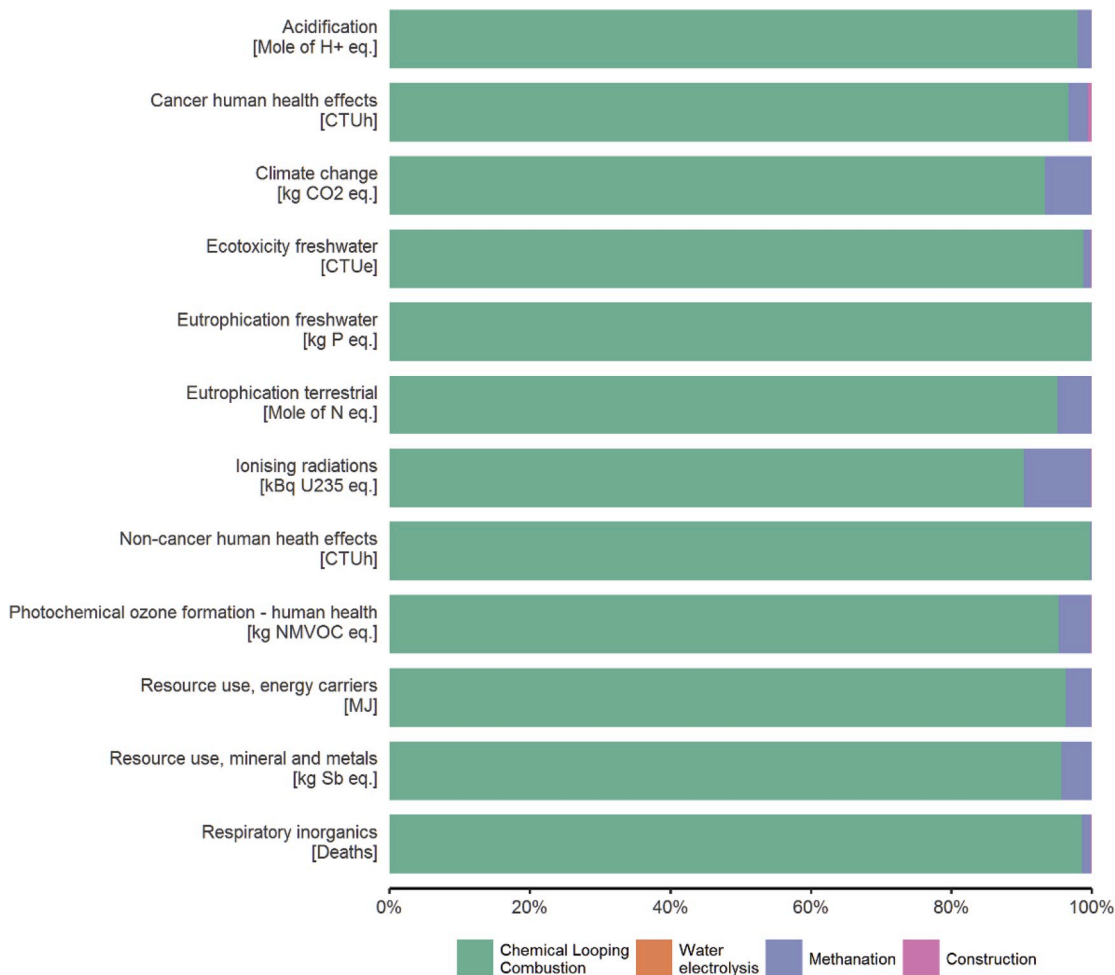
Fig. 6. Hot-spot analysis of the proposed process layout. The label "Construction" includes construction of all units.

fully oxidize all of the carbon content of the fuel is actually released at the same time. Fig. 7 extends the comparative analysis reported in Fig. 5 to three additional scenarios where increasing fractions (arbitrarily set to 11%, 22%, and 33%) of the oxygen produced in PEM units are available to be used in the t-FR, resulting in increasing reductions of the amount of oxygen carrier needed (namely, about 30%, 60%, and 90%).

The chart shows that exploitation of the HP-PEM produced oxygen exploitation can yield substantial improvements in the environmental performances of the proposed layout. At 11%, the proposed system performs better than the reference one not only with respect to climate change and ionizing radiations impacts (as in the case without oxygen feeding, see Fig. 5), but also with respect to the category respiratory inorganics. Further increasing the percentage of PEM-produced oxygen directly fed to the t-FR up to 22%, the proposed layout performs better than the reference system also with respect to acidification, marine eutrophication, and photochemical ozone formation impact categories. Finally, when a 33% of oxygen exploitation is considered, better performances than those of the reference system in all impact categories with the exception of depletion of energy carriers, minerals and metals, and carcinogenic impacts due to toxic pollutants are achieved. The environmental performances of the reference case with respect to these latter impact categories cannot be approached by the proposed system, unless alternative, more sustainable carriers were developed.

The LCA study has two main limitations. First, the study did not consider the decommissioning of the units in the Foreground system (Section 2.3); however, because the construction phase has minimal contributions to the environmental impacts (see Fig. 6), it is expected

that the decommissioning also has minimal contributions. Second, the results could not be compared with literature data; this is because no similar studies, *i.e.* that combine a Chemical Looping Combustion with a Power-to-Methane system, could be found in the literature.

4. Conclusions

This work presented an innovative process layout that integrates Chemical Looping Combustion of solid fuels and a Power-to-Methane system, based on hydrogen production through water electrolysis by means of Polymer Electrolysis Membrane driven by electricity from renewable energies, to achieve a net power production with near-zero CO_2 emissions while simultaneously producing methane. The core of the layout is a multiple interconnected fluidized bed system equipped with a two-stage fuel reactor, a riser used as Air Reactor, a cyclone, a L-valve return leg, and a loop-seal.

A coupled hydrodynamic and kinetic model was applied to evaluate the flue gas composition and flow rate, and the power production of the CLC system. The performance of the hydrogen production unit was evaluated considering data from commercially available units, while that of the methanation unit by developing a thermodynamic calculation method based on minimization of the free Gibbs energy. Both the technical and environmental performance of the system were investigated in the paper. Technical performance was assessed evaluating the thermal power generated by MFB and methanation units, the number of electrolysis cells required to produce hydrogen, CH_4 flow rate, and energy conversion efficiency. Environmental performance was evaluated
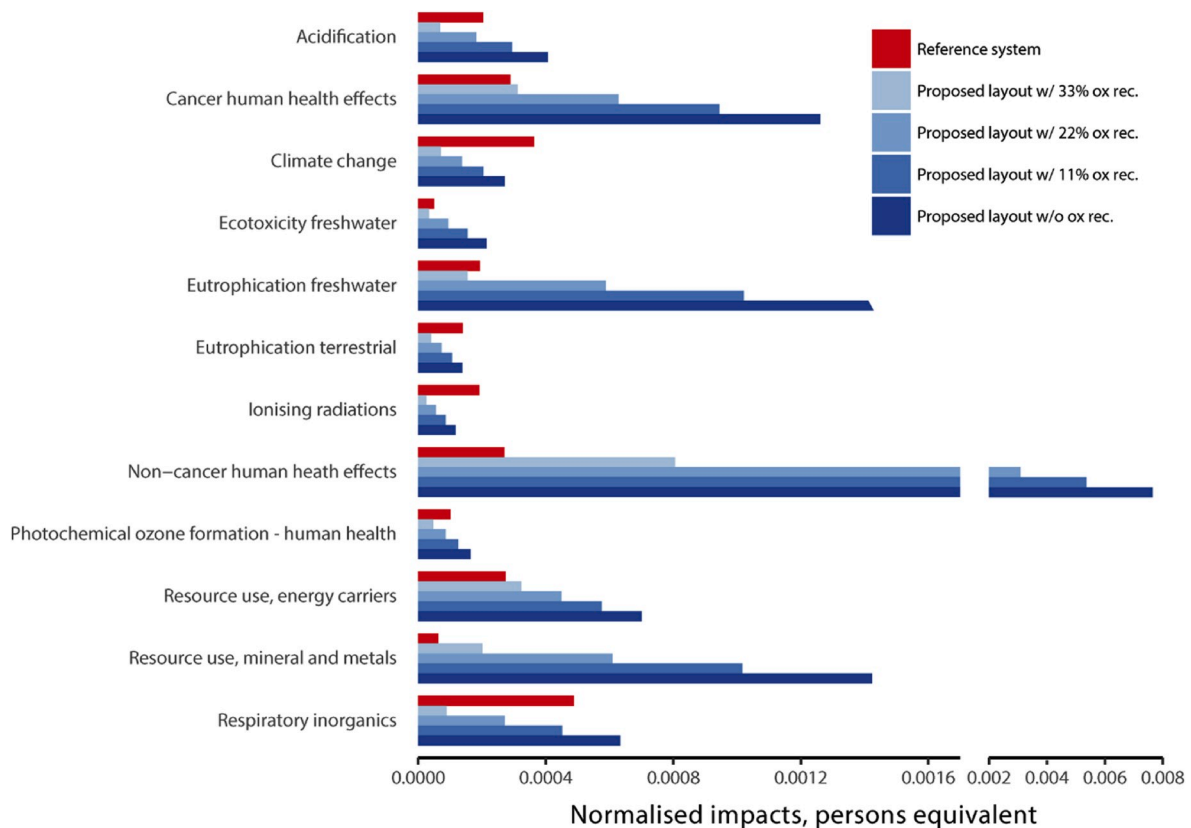
Fig. 7. Normalized environmental impacts of the reference system, the proposed process, and scenarios for PEM-produced oxygen exploitation.

using the Life Cycle Assessment (LCA) methodology.

The proposed system produces, with respect to 1 kg/h of fuel fed, a net thermal power of 4.3 kW/s and a high purity ($C_{CH4} > 95\%$) methane stream equal to $3.3\ 10^{-4}\ Nm^3/h$ with near-zero CO_2 emissions (around $8\ 10^{-8}\ Nm^3/h$). By considering that only energy from renewable sources was fed to the hydrogen production unit, it was assessed the capability of the proposed process to be used as an energy storage system. The estimated electric energy storage efficiency equates 16%.

The LCA study shows that production and disposal of the oxygen carrier used in the Chemical Looping Combustion reactor represents the largest source of the environmental impacts, with contributions ranging from 90% up to ~100% in all the impact categories. The environmental performance of the system with respect to a reference system that includes the conventional pathways to generate electricity and produce methane thus strongly depends on the lifetime amount of oxygen carrier required. The comparison shows that the proposed layout is environmentally preferable to the reference system only with respect to climate change and ionizing radiations impacts. However, when 33% of PEM-produced oxygen is available to be fed to the Chemical Looping Combustion reactor, the proposed layout becomes environmentally preferable with respect to all environmental categories with the exception of depletion of minerals and metals, and energy carriers, and cancer human health effects.

Possible strategies to improve the environmental impacts should therefore focus on further reducing (to ~0, theoretically) the amount of oxygen carrier required and/or on developing alternative OC that are more environmentally sustainable.

Declaration of competing interest

The authors declare that they have no known competing financial interests or personal relationships that could have appeared to influence the work reported in this paper.

Credit authorship statement

P. Bareschino: Conceptualization, Investigation, Software, Visualization, Writing - original draft, Writing - review & editing, Supervision, **E. Mancusi:** Conceptualization, Software, Writing - review & editing, **M. Urciuolo:** Writing - review & editing, **A. Paulillo** Investigation, Software, Writing - original draft, Writing - review & editing, **R. Chirone** Visualization, Writing - original draft, Writing - review & editing, **F. Pepe:** Writing - review & editing.

Declaration of competing interest

The authors declare that they have no known competing financial interests or personal relationships that could have appeared to influence the work reported in this paper.

Appendix A. Supplementary data

Supplementary data to this article can be found online at https://doi.org/10.1016/j.rser.2020.109962.

References

[1] World Resources Institute. Climate analysis indicators tool. 2019.

[2] Eurostat. European statistics. 2017. http://ec.europa.eu/eurostat. [Accessed 30 June 2019].

[3] Götz M, Lefebvre J, Mörs F, McDaniel Koch A, Graf F, Bajohr S, et al. Renewable Power-to-Gas: a technological and economic review. Renew Energy 2016. https://doi.org/10.1016/j.renene.2015.07.066.

[4] Leung DYC, Caramanna G, Maroto-Valer MM. An overview of current status of carbon dioxide capture and storage technologies. Renew Sustain Energy Rev 2014. https://doi.org/10.1016/j.rser.2014.07.093.

[5] Russo ME, Bareschino P, Olivieri G, Chirone R, Salatino P, Marzocchella A. Modeling of slurry staged bubble column for biomimetic CO_2 capture. Int J Greenh Gas Control 2016;47. https://doi.org/10.1016/j.ijggc.2016.01.045.

[6] Diglio G, Bareschino P, Mancusi E, Pepe F. Numerical assessment of the effects of carbon deposition and oxidation on chemical looping combustion in a packed-bed reactor. Chem Eng Sci 2017;160:85–95. https://doi.org/10.1016/j.ces.2016.11.020.

[7] Bareschino P, Solimene R, Chirone R, Salatino P. Gas and solid flow patterns in the loop-seal of a circulating fluidized bed. Powder Technol 2014;264:197–202. https://doi.org/10.1016/j.powtec.2014.05.036.

[8] Mattisson T, Lyngfelt A, Leion H. Chemical-looping with oxygen uncoupling for combustion of solid fuels. Int J Greenh Gas Control 2009. https://doi.org/10.1016/j.ijggc.2008.06.002.

[9] Gayán P, Adánez-Rubio I, Abad A, De Diego LF, García-Labiano F, Adánez J. Development of Cu-based oxygen carriers for chemical-looping with oxygen uncoupling (CLOU) process. Fuel 2012. https://doi.org/10.1016/j.fuel.2012.01.021.

[10] Rönsch S, Schneider J, Matthischke S, Schlüter M, Götz M, Lefebvre J, et al. Review on methanation - from fundamentals to current projects. Fuel 2016;166:276–96. https://doi.org/10.1016/j.fuel.2015.10.111.

[11] Terna. Piano di Sviluppo 2020. 2020.

[12] ISO. Environmental management - life cycle assessment - requirements and guidelines. 2006. EN ISO 14044:2006.

[13] ISO. Environmental management - life cycle assessment - principles and framework. 2006. EN ISO 14040:2006.

[14] Coppola A, Solimene R, Bareschino P, Salatino P. Mathematical modeling of a two-stage fuel reactor for chemical looping combustion with oxygen uncoupling of solid fuels. Appl Energy 2015;157:449–61. https://doi.org/10.1016/j.apenergy.2015.04.052.

[15] Solsvik J, Haug-Warberg T, Jakobsen HA. Implementation of chemical reaction equilibrium by Gibbs and Helmholtz energies in tubular reactor models: application to the steam-methane reforming process. Chem Eng Sci 2016. https://doi.org/10.1016/j.ces.2015.10.011.

[16] Linstrom PJ, Mallard WG. NIST Chemistry webBook, NIST standard reference database number 69. Natl Inst Stand Technol; 2014. citeulike-article-id:3211271.

[17] Perry RH, Green DW. Perry's chemical engineers' handbook. eighth ed. 2013. https://doi.org/10.1017/CBO9781107415324.004.

[18] Ferrero D, Lanzini A, Santarelli M, Leone P. A comparative assessment on hydrogen production from low- and high-temperature electrolysis. Int J Hydrogen Energy 2013;38:3523–36. https://doi.org/10.1016/j.ijhydene.2013.01.065.

[19] Clift R, Doig A, Finnveden G. The application of life cycle assessment to integrated solid waste management. Part 1 - methodology. Process Saf Environ Protect 2000;78:279–87. https://doi.org/10.1205/095758200530790.

[20] Wernet G, Bauer C, Steubing B, Reinhard J, Moreno-Ruiz E, Weidema B. The ecoinvent database version 3 (part I): overview and methodology. Int J Life Cycle Assess 2016;21:1218–30. https://doi.org/10.1007/s11367-016-1087-8.

[21] Zhang X, Bauer C, Mutel CL, Volkart K. Life Cycle Assessment of Power-to-Gas: approaches, system variations and their environmental implications. Appl Energy 2017;190:326–38. https://doi.org/10.1016/j.apenergy.2016.12.098.

[22] Mistry M, Gediga J, Boonzaier S. Life cycle assessment of nickel products. Int J Life Cycle Assess 2016;21:1559–72. https://doi.org/10.1007/s11367-016-1085-x.

[23] Thorne RJ, Bouman EA, Sundseth K, Aranda A, Czakiert T, Pacyna JM, et al. Environmental impacts of a chemical looping combustion power plant. Int J Greenh Gas Control 2019;86:101–11. https://doi.org/10.1016/j.ijggc.2019.04.011.

[24] Fazio S, Castellani V, Salasa S, Schau E, Secchi M, Zamporti L, et al. Supporting information to the characterisation factors of recommended EF Life Cycle Impact Assessment method. 2018.

[25] JRC. Product environmental footprint category rules guidance. 2018., Version 6.3.

[26] Hauschild MZ, Rosenbaum RK, Olsen SI. Life cycle assessment: theory and practice. Springer International Publishing; 2017. https://doi.org/10.1007/978-3-319-56475-3.

[27] Sala S, Cerutti AK, Pant R. Development of a weighting approach for the environmental footprint. Publ Off Eur Union Luxemb; 2018.

[28] Diglio G, Bareschino P, Mancusi E, Pepe F, Montagnaro F, Hanak DP, et al. Feasibility of CaO/CuO/NiO sorption-enhanced steam methane reforming integrated with solid-oxide fuel cell for near-zero-CO2 emissions cogeneration system. Appl Energy 2018. https://doi.org/10.1016/j.apenergy.2018.08.118.